Protective effects of hypericin against infectious bronchitis virus induced apoptosis and reactive oxygen species in chicken embryo kidney cells

Huijie Chen,[*,†,1] Rui Feng,[*,1] Ishfaq Muhammad,[*] Ghulam Abbas,[*] Yue Zhang,[*] Yudong Ren,[‡] Xiaodan Huang,[*] Ruili Zhang,[*] Lei Diao,[†] Xiurong Wang,[§] and Guangxing Li[*,2]

[*]*Key Laboratory for Laboratory Animals and Comparative Medicine of Heilongjiang Province, College of Veterinary Medicine, Northeast Agricultural University, Harbin 150030, China;* [†]*College of Biological and Pharmaceutical Engineering, Jilin Agriculture Science and Technology College, Jilin 132101, China;* [‡]*College of Electrical and Information, Northeast Agricultural University, Harbin 150030, China; and* [§]*State Key Laboratory of Veterinary Biotechnology, Harbin Veterinary Research Institute, Chinese Academy of Agricultural Sciences, Harbin 150001, China*

ABSTRACT   Avian infectious bronchitis virus (IBV), a coronavirus, causes infectious bronchitis leading to enormous economic loss in the poultry industry worldwide. Hypericin (HY) is an excellent compound that has been investigated in antiviral, antineoplastic, and antidepressant. To investigate the inhibition effect of HY on IBV infection in chicken embryo kidney (CEK) cells, 3 different experimental designs: pre-treatment of cells prior to IBV infection, direct treatment of IBV-infected cells, and pre-treatment of IBV prior to cell infection were used. Quantitative real-time PCR (qRT-PCR), immunofluorescence assay (IFA), flow cytometry, and fluorescence microscopy were performed and virus titer was determined by $TCID_{50}$. The results revealed that HY had a good anti-IBV effect when HY directly treated the IBV-infected cells, and virus infectivity decreased in a dose-dependent manner. Furthermore, HY inhibited IBV-induced apoptosis in CEK cells, and significantly reduced the mRNA expression levels of Fas, FasL, JNK, Bax, Caspase 3, and Caspase 8, and significantly increased Bcl-2 mRNA expression level in CEK cells. In addition, HY treatment could decrease IBV-induced reactive oxygen species (ROS) generation in CEK cells. These results suggested that HY showed potential antiviral activities against IBV infection involving the inhibition of apoptosis and ROS generation in CEK cells.

Key words: hypericin, infectious bronchitis virus, apoptosis, reactive oxygen species, chicken embryo kidney cells

INTRODUCTION

Avian infectious bronchitis virus (**IBV**), a member of the *Coronaviridae* family (Cook et al., 2012), causes mild-to-acute respiratory disease in chickens (Benyeda et al., 2009; Westerbeck and Machamer, 2019). IBV infects chickens via the respiratory tract, from which it can spread to other epithelial tissues. Therefore, IBV not only injures the respiratory tract, but also causes damage to the digestive system and urogenital system, such as the proventriculus, kidney, ovary, and oviduct, resulting in respiratory disease, interstitial nephritis, and dysplasia of the oviduct (Zhong et al., 2016). IBV has led to severe economic losses in the poultry industry worldwide. It has been demonstrated that IBV not only causes direct loss due to high mortality, secondary bacterial infection, poor meat production, and egg quality, but also indirect losses arises from increasing drug costs and vaccination in IBV prevention (Liang et al., 2019).

There are multiple known strains of IBV, and increasing numbers of variants have emerged continuous recombinations, resulting in more diversified and complicated genotypes and serotypes (Feng et al., 2015; Laconi et al., 2019). Because of poor vaccine cross protection among different virus serotypes, it makes difficult to prevent and control IBV infection with the current precautionary measures (Mo et al., 2013; Yan et al., 2018). Thus, finding effective antiviral drugs or agents is imperative for alternative approach to prevent IBV infection.

The Chinese government has prohibited the use of antiviral drugs in food animals. Thus, utilization of traditional herbs remains a major focus in antiviral research. Several reports have confirmed that traditional Chinese herbs could effectively inhibit the replication of various viruses (Chen et al., 2018; Dziewulska et al., 2018; Lv et al., 2019; Xie et al., 2017). Hypericin (**HY**), a natural

polycyclic quinone, is mainly extracted from St John's Wort (*Hypericum perforatum L.*) (Barnes et al., 2019). Hypericin has traditionally been used in a wide range of medical applications such as anti-virus (Birt et al., 2009; Marrelli et al., 2014; Naesens et al., 2006; Wolfle et al., 2014), anti-tumor (Mirmalek et al., 2015), and anti-depressant (Zhai et al., 2015). Hypericin has virucidal activity against both DNA and RNA viruses with lipid envelope (Tang et al., 1990), suggesting that HY has the potential to be developed and used as antiviral drugs. In particular, HY has been found to have significant inhibitory effect on HIV infection (Taher et al., 2002). Recent studies on the use of HY for inhibiting hepatitis C virus (**HCV**) have attracted more attention (Jacobson et al., 2001; Shih et al., 2018). Hepatitis C virus infection could induce oxidative stress and endoplasmic reticulum stress, which enhanced the production of reactive oxygen species (**ROS**) and promoted caspase 3 activity, and finally led to hepatocyte injury in vivo and in vitro (Ríos-Ocampo et al., 2019).

Similar to HCV, IBV is also an enveloped single-stranded positive-sense RNA virus, whether HY has the likely inhibitory effect on IBV has not been explored. The aim of this study is to elucidate the antiviral activity and related mechanism of HY inhibiting IBV replication in chicken embryo kidney (**CEK**) cells, and provide alternative approach to prevent and treat IBV infection. The impact of HY on relative mRNA expression levels of IBV, apoptosis-related genes (including Fas, FasL, JNK, Bax, Bcl-2, Caspase 3, and Caspase 8), and ROS production in IBV-infected CEK cells were studied. Our results clearly demonstrated HY had potential antiviral activities against IBV infection involving the inhibition of apoptosis and ROS generation in CEK cells.

MATERIALS AND METHODS

Virus and Cell Cultures

Experimental procedures were approved by the Institutional Animal Ethical Committee of Northeast Agricultural University (Number SRM-08). All animal studies were complied with the animal experiment guidelines of the Animal Experimentation Ethics Committee of Northeast Agricultural University.

The IBV M41 strain was kept at Veterinary Pathology Lab, College of Veterinary Medicine, Northeast Agricultural University, and propagated in 10-day-old specific pathogen-free (**SPF**) chicken embryos (Harbin Veterinary Research Institute, Chinese Academy of Agricultural Sciences). The allantoic fluid of infected embryos was harvested at 72 h post inoculation, and confirmed no other pathogens detected with reverse transcription polymerase chain reaction (**RT-PCR**) and bacterial culture, and finally stored at $-80°C$ until use.

Primary cultures of CEK cells from 18-day-old SPF chicken embryos (Harbin Veterinary Research Institute, CAAS) were prepared according to standard techniques. The cells were cultured in M199 medium (Thermo Fisher Scientific, Waltham, MA, USA) supplemented with penicillin-streptomycin and 10% fetal bovine serum at $37°C$ with 5% CO_2 to allow the formation of cell monolayers in cell culture plates.

Reagents and Antibodies

Hypericin powder (Sigma, St. Louis, MO) with purity 99% was determined by high performance liquid chromatography. A total of 20 mg HY was pre-dissolved in 500 µL dimethylsulfoxide (DMSO, Sigma) and then added 4.5 mL M199 medium as HY stock solution, in which HY concentration is 4,000 µg/mL, and DMSO concentration is 10% (V/V). The stock solution of HY (4.0 mg/mL) was stored at $-20°C$ in the dark. Ribavirin (**RT,** H51023508) was from Sichuan Biokin Pharmaceutical Co., Ltd. (Chengdu, China). N-Acetyl cysteine (**NAC**) and $2'7'$-dichlorofluorescein diacetate (**DCFH-DA**) were obtained from Sigma (St. Louis, MO, USA). Annexin V-FITC kit was purchased from Shanghai Beyotime Biotechnology Co., Ltd. (Shanghai, China). The apoptosis promoter **PAC**-1 (MCE, Brea, CA, USA) and anti-apoptotic **Z-VAD-FMK** (MCE, Brea, CA, USA) were prepared into 10 mM solution with DMSO and stored at $-20°C$. Fluorescein isothiocyanate (**FITC**)-conjugated affiniPure goat anti-rabbit IgG was purchased from Zhongshan Company (Beijing, China). Anti-IBV polyclonal antibody was prepared and kept in Veterinary Pathology Laboratory, College of Veterinary Medicine of Northeast Agricultural University, which could specifically react with IBV.

Cytotoxicity Assay

The cytotoxicity assays were performed according to published 3-(4,5-dimethylthiazol-2-yl)-2,5-diphenyltetrazolium bromide (**MTT**) protocols with minor modifications (Sui et al., 2010). Cell monolayers plated onto 96-well culture plates were washed 3 times with D-Hanks solution. Hypericin at concentrations of 3.125, 6.25, 12.5, 25, 50, 100, 200, and 400 µg/mL were added onto the wells (3 wells per each dilution). Control cells were incubated with the same corresponding concentrations of DMSO solutions as negative controls. The cells were cultured at $37°C$ for 48 h, and the supernatant was taken out and washed 3 times with D-Hanks solution, then 20 µL of MTT solution (5 mg/mL in M199 medium) was added to each well and incubated for 4 h at $37°C$. After washing with D-Hanks solution, 200 µL of DMSO was added to each well. The plates were shaken gently for 15 min to dissolve the formazan precipitate, and the OD570 was recorded. Cell survival rates were calculated from mean values according to the following equation: (OD570 drug)/(OD570 control) $\times$ 100%.

Table 1. Sequences of primers used for the qRT-PCR assays.

| Gene	Primer sequence (5′-3′)	Amplicon size (bp)	Annealing temperature (°C)	Accession number
IBV	F: CAAGCTAGGTTTAAGCCAGGT R: TCTGAAAACCGTAGCGGATAT	189	58.3	FJ904723.1
Fas	F: CTTCCACCTGCTCCTCGTCATTG R: TTCGTGCAGCACTGACCACTG	174	58.5	NM_001199487.1
FasL	F: CCTTCACCAGTGGCATTCAGTACC R: CCTCGTTGTCACAGTGCCTTCC	100	58.0	AY765397.1
JNK	F: GTTTCCTGATTCTCTCTTCC R: CTCCTCAATGGTGTGCTC	215	61.5	NM_001318225.3
Bax	F: ACTCTGCTGCTGCTCTCCTCTC R: ATCCACGCAGTGCCAGATGTAATC	151	58.1	XM_025145468.1
Bcl-2	F: GAGTTCGGCGGCGTGATGTG R: TTCAGGTACTCGGTCATCCAGGTG	69	60.0	NM_205339.2
Caspase 3	F: CCACCGAGATACCGGACTGT R: AACTGCTTCGCTTGCTGTGA	157	61.3	NM_204725.1
Caspase 8	F: GGAAGCAGTGCCAGAACTCAGAAG R: TTGTTGTGGTCCATGCACCGATAG	151	61.0	AY057939.2
β-actin	F: ATTGCTGCGCTCGTTGTT R: CTTTTGCTCTGGGCTTCA	189	60.0	K02173.1
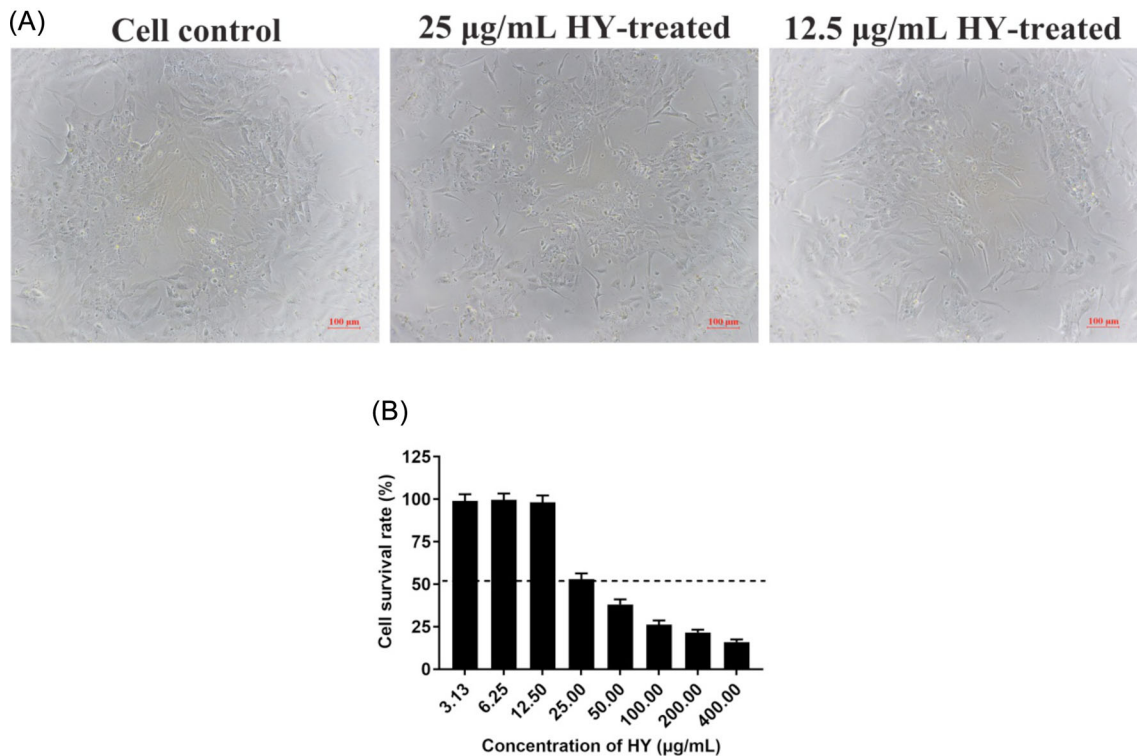
Figure 1. Effect of HY on the viability of CEK cells. (A) Trypan blue staining was used to assess cell viability. The 25 and 12.5 µg/mL HY-treated CEK cells and the control CEK cells were stained with trypan blue. Cells not stained with trypan blue are considered viable. (B) Cell viability was determined by MTT colorimetric assay. The survival rates of CEK cells was given at different concentrations of HY, and cell survival rates of more than 50% (above the dotted line) was considered to be the maximum non-toxic concentration of HY. CEK = chicken embryo kidney; HY = hypericin. Data are expressed as mean $\pm$ SD of 3 independent experiments (t-test, *p < 0.05, **p < 0.01).

Antiviral Activity Assays

Pre-treatment of Cells Prior to IBV Infection
To analyze the impact of HY on cell to inhibit IBV infection, the CEK cells cultured on 96-well plates were treated with continuous multiple dilutions of HY solutions in serum-free M199 medium, at 37°C for 1 h and then washed 3 times with D-Hanks solution. The cells were subsequently infected with IBV (100 **TCID$_{50}$**) and cultured at 37°C for 30 h. The cell samples were repeatedly frozen and thawed 3 times, extracted to obtain total RNAs, and reverse transcribed into cDNA. The relative mRNA expression levels of IBV N gene was detected with quantitative real-time RT-PCR (**qRT-PCR**). In addition, the virus titer of the cell samples was determined by TCID$_{50}$ according to conventional
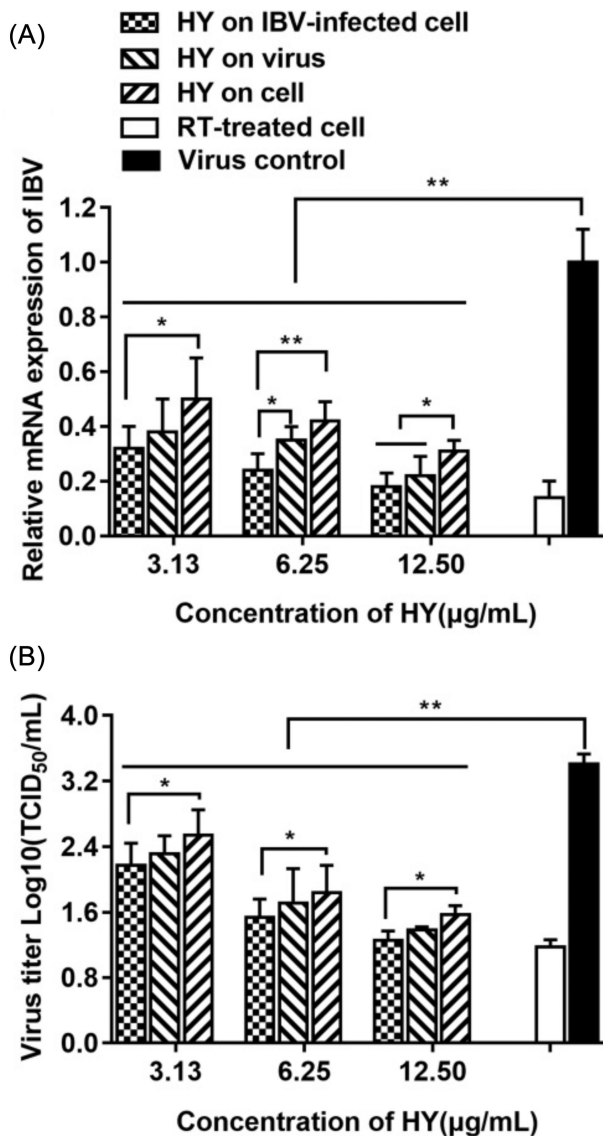
Figure 2. The impact of HY on the relative mRNA expression levels of IBV N gene and virus titer in CEK cells. In 3 different HY treatment group of pre-treatment cells prior to IBV infection, direct treatment of IBV-infected cells, and pre-treatment IBV prior to cell infection, the relative mRNA expression levels of IBV-N gene (2A) and the virus titer (2B) were detected, respectively. IBV-infected CEK cells and 10 μg/mL RT-treated CEK cells after IBV infection were included as controls. CEK = chicken embryo kidney; HY = hypericin; RT = ribavirin. Data are expressed as mean $\pm$ SD of 3 independent experiments (t-test, $*p < 0.05$, $**p < 0.01$).

procedures. Meanwhile, the 10 µg/mL RT-treated cells after IBV infection and IBV-infected CEK cells were processed as controls.

Direct Treatment of IBV-infected Cells To determine the effect of HY on IBV-infected cells, the CEK cells cultured on 96-well plates were infected with 100 $TCID_{50}IBV$ for 1 h at 37°C, and then treated with continuous multiple dilutions of HY solutions at 37°C for 30 h. According to the above description, the relative mRNA expression levels of IBV N gene and virus titer were detected.

Pre-treatment of IBV Prior to Cell Infection To investigate direct effects of HY on the virus, 100

$TCID_{50}IBV$ was incubated with continuous multiple dilutions of HY solutions at 37°C for 1 h. The HY-treated IBV was subsequently used to infect CEK cells at 37°C for 30 h. As described above, the relative mRNA expression levels of IBV N gene and virus titer were detected.

Immunofluorescence Assay (IFA)

In the above 3 experimental designs, the best way of antiviral effect of HY on IBV was selected, and IBV multiplication in CEK cells was detected with indirect immunofluorescence assay (**IFA**). After washing with D-Hanks solution, the 3.125, 6.25, and 12.5 µg/mL of HY directly treated IBV-infected cells were fixed with 4% paraformaldehyde in PBS followed by quenching with 0.1% glycine in PBS and 1% Triton-X100 for 10 min. After washing, the cells were incubated with rabbit anti-IBV antibody (1:200) for 1 h followed by incubation with fluorescence-conjugated goat anti-rabbit IgG (1:500) for 30 min in the dark. The fluorescent images were examined under a Ti-S fluorescence microscope (Nikon, Tokyo, Japan). Additionally, 10 µg/mL RT-treated CEK cells after IBV infection, IBV-infected CEK cells, and mock CEK cells were detected as controls.

Cell Apoptosis Analysis

In total, 2 approaches were used to evaluate the effect of HY on cell apoptosis as described previously (Singh et al., 2019). In brief, 100 TCID50 IBV-infected CEK cells treated with 12.5 µg/mL HY were cultured at 37°C for 30 h. Then, the apoptotic cells were analyzed using an Annexin V-FITC kit as described previously (Leber et al., 2018). The 20 µM PAC-1-treated CEK cells, 20 µM Z-VAD-FMK-treated CEK cells followed with IBV infection, IBV-infected CEK cells, and mock CEK cells were prepared and assayed concurrently. Moreover, flow cytometry was used to quantify the number of Annexin V and propidium iodide-stained cells among different experimental groups. In brief, the IBV-Infected cells were treated with 12.5 µg/mL HY as above and trypsinated. The viable cells determined with trypan blue staining were adjusted to a final density of 4×10^5 cells/mL. Then the cells were incubated with FITC-conjugated anti-Annexin V antibody and propidium iodide for 15 min in the dark prior to flow cytometry analysis. The IBV-infected CEK cells and mock CEK cells were tested as controls.

RNA Extraction and Reverse Transcription

The total RNAs of different experimental groups were extracted using a Universal RNA Extraction Kit (Thermo Fisher Scientific, Waltham, MA, USA) according to the manufacturer's instructions. All the concentrations and the A260/A280 ratios of extracted RNA samples were measured using NanoDrop 2000 spectrophotometer (Thermo Fisher Scientific,
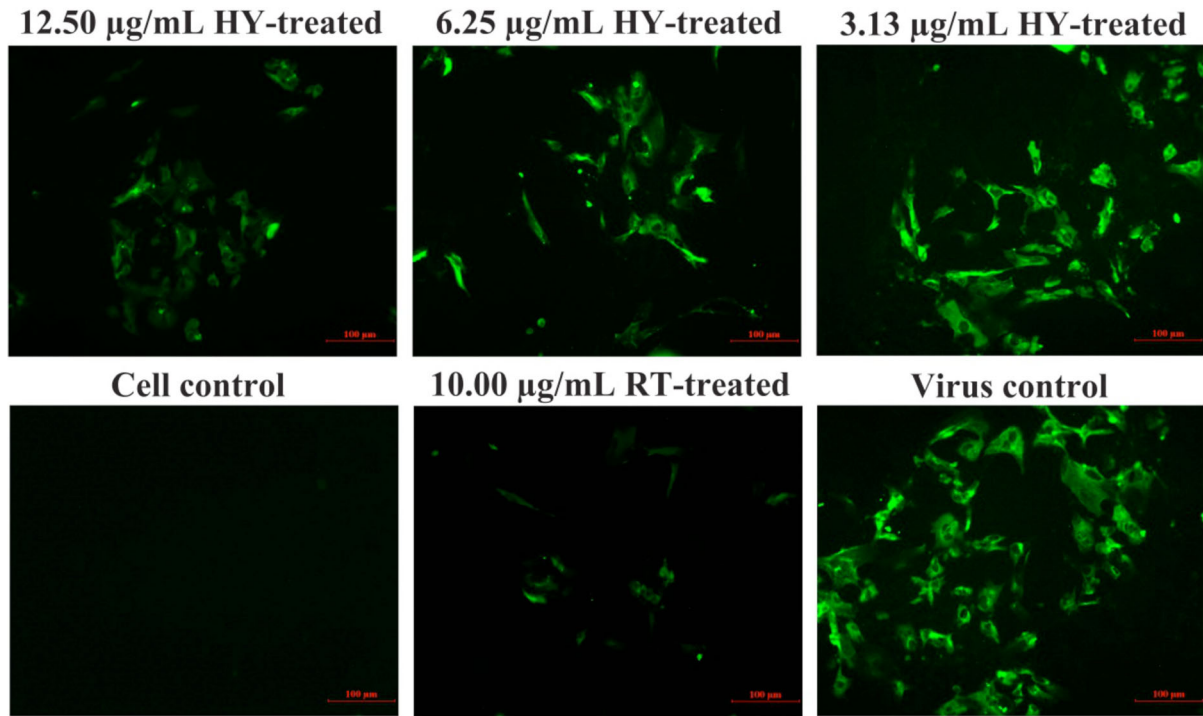
Figure 3. Inhibitory effects of HY on IBV infection detected by immunofluorescence assays. The CEK cells were infected with 100 TCID$_{50}$ IBV for 1 h at 37°C followed by incubation with serially diluted HY at concentrations of 3.125, 6.25, and 12.5 µg/mL for 30 h. The IBV-infected CEK cells, 10 µg/mL RT-treated CEK cells after IBV infection and mock CEK cells were included as controls, respectively. Fluorescence intensity (20×) is proportional to viral infectivity and inversely related to the treatments with different concentrations of HY. CEK = chicken embryo kidney; HY = hypericin; RT = ribavirin.

Waltham, MA, USA), and agarose gel electrophoresis was used to assay the integrity of the extracted RNA. The total RNAs were reverse transcribed into cDNAs using moloney murine leukemia virus reverse transcriptase and oligo (dT) (Takara Bio Inc., Dalian, China) with PCR instrument (TaKaRa, Japan) and stored at −20°C for the following qRT-PCR assay.

Quantitative Real-Time PCR (qRT-PCR)

The mRNA expression levels of target genes were determined, including IBV N gene, Fas, FasL, JNK, Bax, Bcl-2, Caspase 3, and Caspase 8 with an applied LightCycler 96 Real-Time PCR System (Roche Molecular Systems, Inc., Schlieren, Switzerland). All primers pairs used for qRT-PCR detection are listed in Table 1. These primers were synthesized by the Genewiz Biological Technology Co., Ltd (Suzhou, China). The relative expression ratios of target genes were calculated using the $2^{-\Delta\Delta Ct}$ method (Yu et al., 2017).

The amplification reaction was conducted containing 2 µL of cDNA, 0.6 µL of each of the forward and reverse primers, 10 µL universal SYBR Green (ROX), and 3.4 µL nuclease free water for a final volume of 20 µL for each reaction. The following thermal profile for the qRT-PCR assays was used in all the primer sets: pre-incubation 1 cycles at 95°C for 600 s, followed by 2 step amplification: 42 cycles at 95°C for 15 s and 60°C for 30 s, followed by melting: 1 cycles at 95°C for 10 s, 65°C

for 60 s and 97°C for 1 s, followed by cooling 1 cycles at 37°C for 30 s.

Detection of Intracellular ROS Production

2′7′-dichlorofluorescein diacetate probe was used to measure the intracellular ROS scavenging activity of HY in IBV-infected cells (Chavez and Pietras, 2018). Briefly, the CEK cells were pre-incubated with IBV for 1 h, followed by incubation with 3.125, 6.25, and 12.5 µg/mL HY for 30 h. The medium was removed and the cells were washed with PBS. Then, the medium containing 10 μM DCFH-DA was added for 30 min at 37°C. After washing with PBS, cells were photographed using a Ti-S fluorescence microscope (Nikon, Tokyo, Japan). And the CEK cells were pre-treated with 1.5 mM NAC before IBV infection as control.

Statistical Analysis

The number of the experiment repetition in all the experiment was 3 times. The experimental data was analyzed with SPSS 17.0 software (SPSS Inc., Chicago, IL). The results were expressed as the means ± standard deviation. Differences between groups were evaluated using the one-way analysis of variance of two-tailed test. P-values of < 0.05 were considered as statistically significant, and P-values of < 0.01 were considered as highly significant.
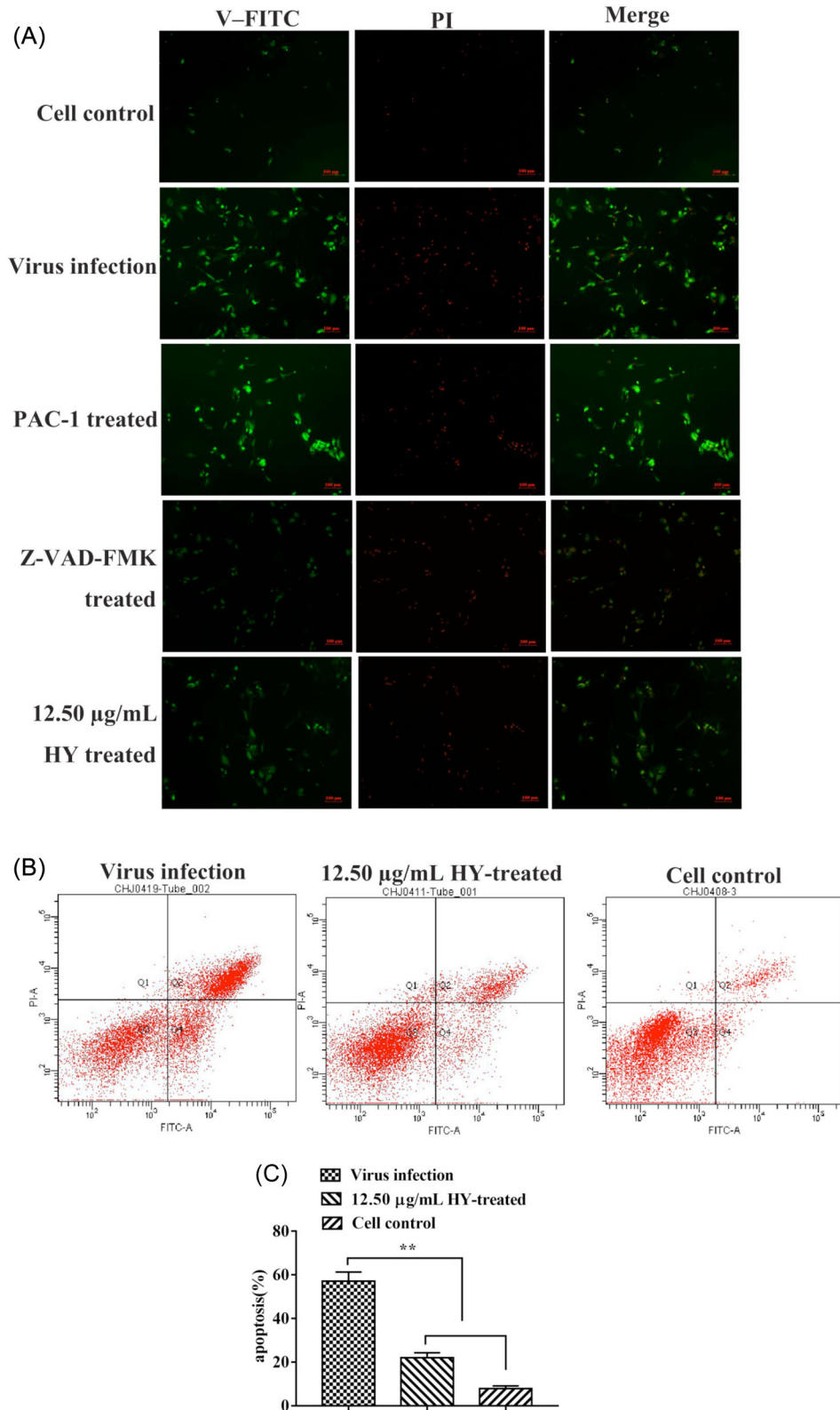
Figure 4. Effect of the HY on apoptosis in IBV-infected CEK cells. (A) The CEK cells were infected with 100 $TCID_{50}$ IBV for 1 h at 37°C followed by incubating 12.5 μg/mL of HY for 30 h. The 20 μM PAC-1-treated CEK cells, 20 μM Z-VAD-FMK pre-treated CEK cells before IBV infection, IBV-infected CEK cells and mock CEK cells were included as control. The green fluorescence signals are designated as the index of early apoptosis in immunofluorescence analysis. Fluorescence intensity (10×) is provided. (B) To quantify the cell apoptosis, the 12.5 μg/mL HY-treated CEK cells after IBV infection, IBV-infected CEK cells and mock CEK cells were stained with Annexin V-FITC and PI, and then analyzed by flow cytometry. Data are presented as dual parameter consisting of Annexin V versus PI. The early apoptosis (Annexin V-FITC staining) and late apoptosis (PI staining) were reflected in Q4 and Q2 gates, respectively. (C) The percentages shown in the column chart are the proportion of apoptotic cells (right panel) in different experimental groups. The differences between means were considered highly significant at **$P < 0.01$ compared with the IBV-infected control group. CEK = chicken embryo kidney; HY = hypericin; PI = propidium iodide.
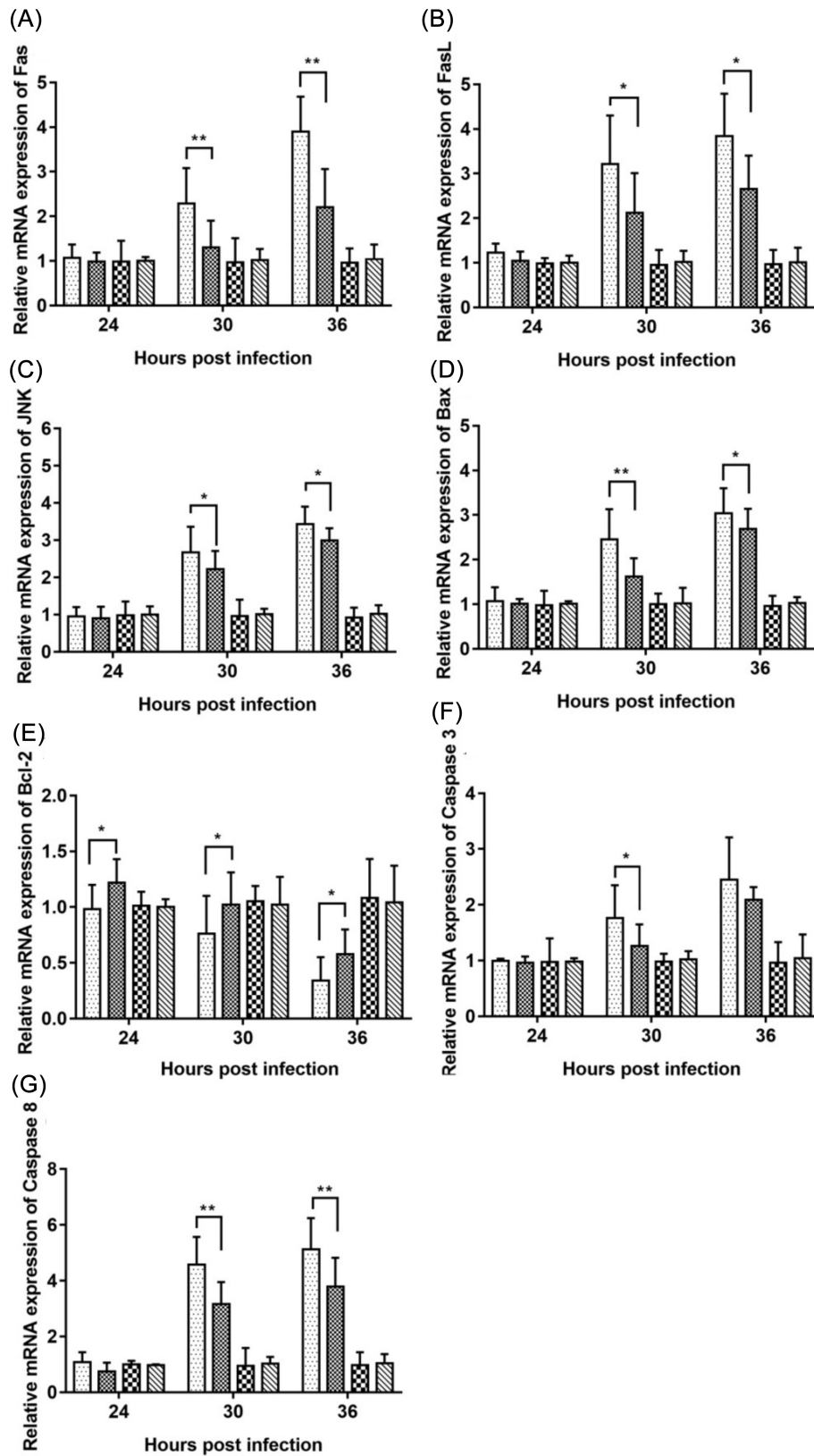
Figure 5. Effects of HY on the mRNA expression level of apoptosis-related genes in vitro. The CEK cells were infected with 100 $TCID_{50}$ IBV for 1 h at 37°C followed by incubation with HY at the concentration of 12.5 µg/mL. The CEK cells were simultaneously cultured with M199 medium as a mock control, and infected with 100 $TCID_{50}$ IBV as a virus control, and treated with HY at a concentration of 12.5 µg/mL as a drug reference, respectively. Total RNA was subsequently extracted from cell lysates at 24, 30, and 36 h after treatment. The relative mRNA expression of Fas (A), FasL (B), JNK (C), Bax (D), Bcl-2 (E), Caspase 3 (F), and Caspase 8 (G) were assessed by RT-qPCR. CEK = chicken embryo kidney; IBV = infectious bronchitis virus; HY = hypericin. The differences between the means were considered significant at *$P < 0.05$ and highly significant at **$P < 0.01$ as compared with the IBV-infected control group.
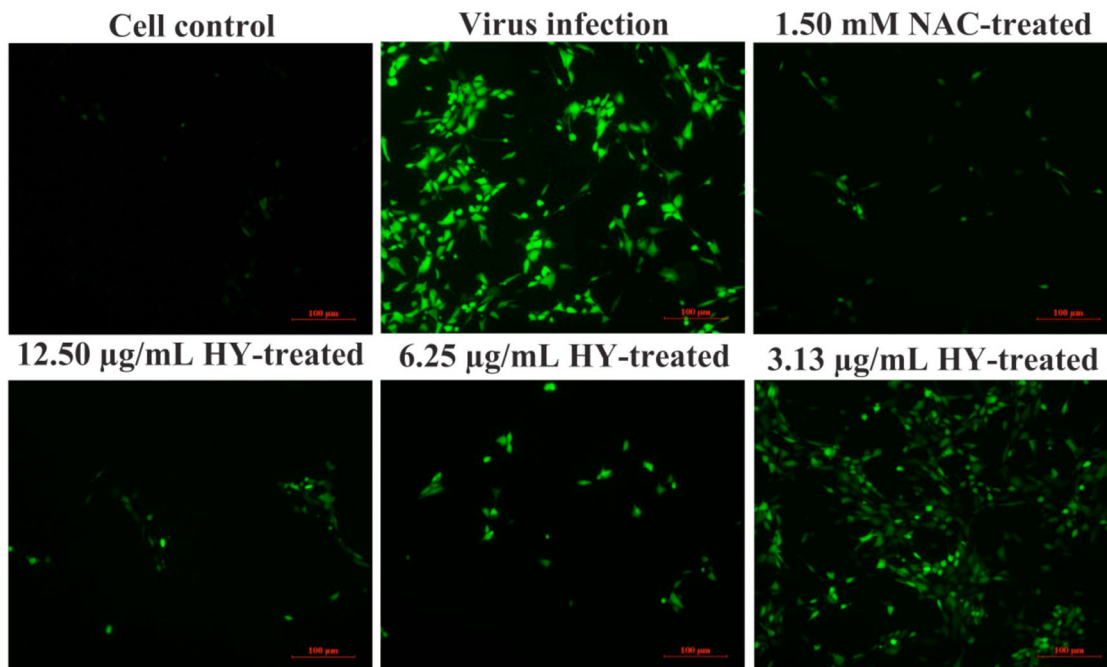
Figure 6. Inhibitory effects of HY on ROS production. The CEK cells were infected with 100 TCID$_{50}$ IBV for 1 h at 37°C followed by incubation with serially diluted HY at concentrations of 3.125, 6.25, and 12.5 μg/mL for 30 h. The CEK cells were simultaneously cultured with M199 medium as a mock control, and infected with 100 TCID$_{50}$ IBV as a virus control, and pre-incubated with 1.5 mM NAC for 1 h before IBV infection as a positive control, respectively. Fluorescence intensity (10×) is proportional to viral infectivity and inversely related to HY concentration. CEK = chicken embryo kidney; HY = hypericin; NAC = N-Acetyl cysteine.

RESULTS

Evaluation of Cytotoxicity of HY

The cell viability indicated by Trypan blue staining was observed under an optical microscope, and further confirmed by MTT assays. The results showed that the maximum nontoxic concentration of HY was 12.5 μg/mL. Trypan blue staining showed that cells survived below 12.5 μg/mL of HY (Figure 1A). Cell proliferation determined by MTT assay had no significant effect and the survival rate was nearly 100% below 12.5 μg/mL of HY (Figure 1B).

Antiviral Effect of HY

The antiviral effect of HY was analyzed by the relative mRNA expression levels of IBV-N gene (Figure 2A) and the virus titer (Figure 2B) in CEK cells. From the Figure 2A, it could be seen that in the 3 experimental designs, the viral mRNA level significantly decreased compared with the virus control, and with the increase of HY concentration, the mRNA level of IBV decreased in a dose-dependent manner. Furthermore, at the same drug concentration, the relative expression levels of the viral mRNA was the lowest when HY directly treated the IBV-infected cells, followed by the group of HY pre-treatment of IBV prior to cell infection, and followed by the group of HY pre-treatment of cells prior to IBV infection.

The virus titers at each group was detected and showed in Figure 2B, with the increase of HY concen-

tration, the titer of IBV decreased gradually. While, at the same drug concentration, the virus titer was the lowest when HY directly treated the infected virus cells, followed by the group of HY pre-treatment virus prior to infection, and followed by the group of HY pre-treatment cells prior to infection.

Meanwhile, the antiviral effect of HY directly treated the IBV-infected cells at the concentration of 12.5 μg/mL, was similar to RT at the concentration of 10 μg/mL (Figure 2). Therefore, HY directly treated the IBV-infected cells was selected to conduct in followed experiments.

IFA Analysis Confirmed the Inhibitory Effect of HY on IBV infection

To further confirm the inhibitory effect of HY on IBV-infected cells, the viral fluorescent signal was detected by IFA (Figure 3). As can be seen from Figure 3, IBV-infected CEK cells generated strong fluorescence signals at 30 h post-infection. In contrast, the fluorescence signals in HY directly treated the IBV-infected cells decreased obviously in a dose-dependent manner. This further confirmed the inhibition effect of HY on IBV-infected cells.

The Effect of HY on IBV-induced Apoptosis

The immunofluorescence results showed that addition of HY to virus-infected cells resulted in fewer apoptotic cells compared with virus infection control

and apoptosis promoter PAC-1 (20 μM) control group, and similar to the apoptosis inhibitor Z-VAD-FMK (20 μM) control group (Figure 4A). The number of apoptotic cells was quantified with flow cytometry. The results showed that there was ∼2.59-fold decrease in the percentage of apoptotic cells at 12.5 μg/mL of HY treatment group compared with virus infection group (Figures 4B and 4C).

The Effect of HY on Relative mRNA Expression of Apoptosis-related Genes

The mRNA expression levels of apoptosis-related genes, including Fas, FasL, JNK, Bax, Bcl-2, Caspase 3, and Caspase 8 were determined. As can be seen from Figure 5, HY treatment significantly reduced the mRNA levels of Fas, FasL, JNK, Bax, Caspase 3, and Caspase 8 genes (Figures 5A−D, 5F, and 5G) after IBV infection at 30 h and 36 h, and significantly increased the mRNA expression levels of Bcl-2 gene after IBV infection at 24 h, 30 h, and 36 h (Figure 5E). These data demonstrated that HY inhibited apoptosis in IBV-infected CEK cells by decreasing the expression of pro-apoptotic genes and increasing anti-apoptotic gene expression. However, no difference could be found in the above detected parameters in the only HY-treated CEK cells compared with those in mock cells.

The Effects of HY on ROS Production

We determined the ROS generation in HY directly treated the IBV-infected cells using DCFH-DA method. As shown in Figure 6, IBV could significantly induce the ROS production, while HY could inhibit the ROS production in IBV-infected CEK cells. And with the increase of HY concentration, the fluorescence signal of ROS decreased in a dose-dependent manner. The effect of inhibiting ROS at 6.25, 12.5 μg/mL of HY treatment was similar to ROS inhibitors NAC.

DISCUSSION

Our results showed that HY could inhibit IBV infection and inhibit apoptosis and production of ROS in CEK cells. It has been reported that there were multiple known strains of IBV, IBV strain M41, is typical respiratory virus, which replicates primarily in the respiratory tract and subsequently spreads and replicates in a range of other tissues (De Wit et al., 2019; Hodgson et al., 2004). The CEK cells are the most susceptible cells of strain M41 *in vitro* (Abdel-Moneim et al., 2009; Zhang et al., 2017). Therefore, we selected M41 strain for infection of CEK cells to study the anti-IBV effect of HY.

In the cytotoxicity assay, MTT assay was performed to measure cell viability. MTT method is a recognized and commonly used method to evaluate the metabolic activity of living cells (Gao et al., 2019; Şueki et al.,

2019). Because HY is low levels of solubility in water (Bianchini et al., 2019; Montanha et al., 2017), it is insoluble in M199 cell culture medium. In MTT assay, HY was pro-dissolved in DMSO first, and diluted to a certain concentration with medium M199. In the process of dilution, the content of DMSO is not more than 1% (Hebling et al., 2015; Şimşek et al., 2015), in order to ensure that DMSO is non-toxic to the cells and to obtain the maximum non-toxic concentration of HY accurately. By observing the cell morphology and calculating the cell survival rate, the maximum non-toxic concentration of HY was 12.50 μg/mL (Figure 1).

A total of 3 different experimental designs: (1) pre-treatment of cells prior to infection; (2) direct treatment of virus-infected cells; and (3) pre-treatment of virus prior to infection were used to analyze the antiviral activity of HY on CEK cells infection by IBV (De La Torre et al., 2011; Yin et al., 2011). Our results showed that direct treatment of HY on virus-infected cells was the best among 3 different experimental designs (Figure 2). In the direct treatment of HY on virus-infected cells, it may be due to the effect of HY on infected cells, effectively inhibited the activity of viral transcriptase, and effectively reduced the replication of IBV in CEK cells. The pre-treatment of HY on IBV prior to infection may be related to the photoperiod and oxygen supply of HY. Under light conditions, HY could absorb photons, and then stimulate singlet oxygen to play an antiviral role. Because this experiment was carried out under the condition of no oxygen and weak light, the direct attack effect of HY on virus particles was not brought into full play, and the killing effect of virus was weakened (Miskovsky, 2002; Xu et al., 2019). In the pre-treatment of HY on cells prior to infection, HY blockaded on the adsorption of virus in CEK cells was weak, or did not protect the cells, thus failed to effectively prevent IBV from entering the host cells (Pu et al., 2009, 2012). Therefore, in the following experiments, the CEK cells were first infected IBV, and then incubated HY solution. To further confirm the inhibitory effect of direct treatment of HY on virus-infected cells, the viral fluorescent signal was detected by IFA (Figure 3). Our results confirmed the inhibition effect of direct treatment of HY on virus-infected cells.

While apoptosis usually functions as a host defense mechanism that ensures killing of infected cells (Elmore, 2007), several viruses, including IBV, have been shown to induce apoptosis to enable efficient virus transmission, while avoiding overt inflammatory responses and activation of the immune system (Zhou et al., 2017). Our results showed that IBV could induce apoptosis in CEK cells (Figure 4), and increase mRNA expression levels of Fas, FasL, JNK, Bax, Caspase 3, and Caspase 8, with the exception of Bcl-2, which significantly decreased after IBV infection (Figure 5), which was consistent with other reports (Chhabra et al., 2016; Fung et al., 2014; Liao et al., 2013). It was found that IBV could increase the mRNA expression levels of Fas, FasL, and Bax, and decrease the mRNA

expression level of Bcl-2 in IBV-infected HD11 cells (Han et al., 2017). Another research demonstrated that JNK served as a pro-apoptotic protein during IBV infection. Interestingly, pro-apoptotic activity of JNK was not mediated via c-Jun, but involved modulation of the anti-apoptotic protein B-cell lymphoma 2 (Bcl2) (Fung and Liu, 2017). Moreover, our results showed that HY could inhibit apoptosis induced by IBV on CEK cells (Figure 4), and reduced mRNA expression levels of Fas, FasL, JNK, Bax, Caspase 3, and Caspase 8, but increased Bcl-2 mRNA expression level after IBV infection (Figure 5). This is similar with human umbilical vein endothelial cells, in which HY could inhibit cell apoptosis by affecting the expression of apoptosis-related genes and inhibit production of ROS (Do and Kim, 2017).

Antioxidant activity of *Hypericum perforatum L.* and its components have been reported (Gioti et al., 2009). Furthermore, the study showed that HY had an antioxidative effect (Cakir et al., 2003). Therefore, we investigated whether HY ameliorated IBV-induced ROS generation. Our results revealed that HY could inhibit ROS production in the absence of phototherapy (Figure 6), which was consistent with other report (Da Silva et al., 2018).

In summary, the present study was the first time to show that HY inhibited IBV infection. Furthermore, anti-IBV effect of HY may be associated with its inhibition of apoptosis and ROS production. HY reduced the mRNA levels of apoptosis-related genes such as Fas, FasL, JNK, Bax, Caspase 3, and Caspase 8, and up-regulated anti-apoptotic gene (Bcl-2) mRNA expression. The data suggest the potential use of HY as antiviral agents against IBV, however, further studies are required to elucidate the molecular mechanism of HY on IBV infection.

ACKNOWLEDGEMENTS

REFERENCES

Abdel-Moneim, A. S., P. Zlotowski, J. Veits, G. M. Keil, and J. P. Teifke. 2009. Immunohistochemistry for detection of avian infectious bronchitis virus strain M41 in the proventriculus and nervous system of experimentally infected chicken embryos. Virol. J. 6:15.

Barnes, J., J. T. Arnason, and B. D. Roufogalis. 2019. St John's wort (*Hypericum perforatum L.*): botanical, chemical, pharmacological and clinical advances. J. Pharm. Pharmacol. 71:1−3.

Benyeda, Z., T. Mato, T. Suveges, E. Szabo, V. Kardi, Z. Abonyi-Toth, M. Rusvai, and V. Palya. 2009. Comparison of the pathogenicity of QX-like, M41 and 793/B infectious bronchitis strains from different pathological conditions. Avian Pathol. 38:449−456.

Bianchini, P., M. Cozzolino, M. Oneto, L. Pesce, F. Pennacchietti, M. Tognolini, C. Giorgio, S. Nonell, L. Cavanna, P. Delcanale, S. Abbruzzetti, A. Diaspro, and C. Viappiani. 2019. Hypericin-apomyoglobin: an enhanced photosensitizer complex for the treatment of tumor cells. Biomacromolecules 20:2024−2033.

Birt, D. F., M. P. Widrlechner, K. D. Hammer, M. L. Hillwig, J. Wei, G. A. Kraus, P. A. Murphy, J. McCoy, E. S. Wurtele, J. D. Neighbors, D. F. Wiemer, W. J. Maury, and J. P. Price. 2009. Hypericum in infection: identification of anti-viral and anti-inflammatory constituents. Pharm. Biol. 47:774−782.

Cakir, A., A. Mavi, A. Yildirim, M. E. Duru, M. Harmandar, and C. Kazaz. 2003. Isolation and characterization of antioxidant phenolic compounds from the aerial parts of *hypericum hyssopifolium L.* by activity-guided fractionation. J. Ethnopharmacol. 87:73−83.

Chavez, J. S., and E. M. Pietras. 2018. Hematopoietic stem cells rock around the clock: circadian fate control via TNF/ROS signals. Cell Stem Cell 23:459−460.

Chen, Y., Y. Yang, X. Yang, F. Yao, K. Ming, W. Yuan, L. Zeng, and J. Liu. 2018. Antiviral effect of baicalin phospholipid complex against duck hepatitis A virus type 1. Poult. Sci. 97:2722−2732.

Chhabra, R., S. V. Kuchipudi, J. Chantrey, and K. Ganapathy. 2016. Pathogenicity and tissue tropism of infectious bronchitis virus is associated with elevated apoptosis and innate immune responses. Virology 488:232−241.

Cook, J. K., M. Jackwood, and R. C. Jones. 2012. The long view: 40 years of infectious bronchitis research. Avian Pathol. 41:239−250.

Da Silva, S. E. L., H. L. Ferreira, A. F. Garcia, F. E. S. Silva, R. Gameiro, C. U. F. Fabri, D. S. Vieira, and T. C. Cardoso. 2018. Mitochondrial bioenergy alterations in avian HD11 macrophages infected with infectious bronchitis virus. Arch. Virol. 163:1043−1049.

De La Torre, J. C., X. Ren, F. Meng, J. Yin, G. Li, X. Li, C. Wang, and G. Herrler. 2011. Action mechanisms of lithium chloride on cell infection by transmissible gastroenteritis coronavirus. PLoS ONE 6:e18669.

De Wit, J. J. S., A. Malo, and J. K. A. Cook. 2019. Induction of IBV strain-specific neutralizing antibodies and broad spectrum protection in layer pullets primed with IBV massachusetts (mass) and 793B vaccines prior to injection of inactivated vaccine containing mass antigen. Avian Pathol. 48:135−147.

Do, M. H., and S. Y. Kim. 2017. Hypericin, a naphthodianthrone derivative, prevents methylglyoxal-induced human endothelial cell dysfunction. Biomol. Ther. 25:158−164.

Dziewulska, D., T. Stenzel, M. Smialek, B. Tykalowski, and A. Koncicki. 2018. An evaluation of the impact of aloe vera and licorice extracts on the course of experimental pigeon paramyxovirus type 1 infection in pigeons. Poult. Sci. 97:470−476.

Elmore, S. 2007. Apoptosis: a review of programmed cell death. Toxicol. Pathol. 35:495−516.

Feng, K., Y. Xue, J. Wang, W. Chen, F. Chen, Y. Bi, and Q. Xie. 2015. Development and efficacy of a novel live-attenuated QX-like nephropathogenic infectious bronchitis virus vaccine in China. Vaccine 33:1113−1120.

Fung, T. S., Y. Liao, and D. X. Liu. 2014. The endoplasmic reticulum stress sensor IRE1alpha protects cells from apoptosis induced by the coronavirus infectious bronchitis virus. J. Virol. 88:12752−12764.

Fung, T. S., and D. X. Liu. 2017. Activation of the c-Jun NH2-terminal kinase pathway by coronavirus infectious bronchitis virus promotes apoptosis independently of c-Jun. Cell Death Dis. 8:3215.

Gao, X., C. Wang, Z. Chen, Y. Chen, R. K. Santhanam, Z. Xue, Q. Ma, Q. Guo, W. Liu, M. Zhang, and H. Chen. 2019. Effects of N-trans-feruloyltyramine isolated from laba garlic on antioxidant, cytotoxic activities and H_2O_2-induced oxidative damage in HepG2 and L02 cells. Food Chem. Toxicol. 130:130−141.

Gioti, E. M., Y. C. Fiamegos, D. C. Skalkos, and C. D. Stalikas. 2009. Antioxidant activity and bioactive components of the aerial parts of *hypericum perforatum L.* from Epirus, Greece. Food Chem. 117:398−404.

Han, X., Y. Tian, R. Guan, W. Gao, X. Yang, L. Zhou, and H. Wang. 2017. Infectious bronchitis virus infection induces apoptosis during replication in chicken macrophage HD11 cells. Viruses 9:E198.

Hebling, J., L. Bianchi, F. G. Basso, D. L. Scheffel, D. G. Soares, M. R. Carrilho, D. H. Pashley, L. Tjäderhane, and C. A. de Souza Costa. 2015. Cytotoxicity of dimethyl sulfoxide (DMSO) in direct contact with odontoblast-like cells. Dent. Mater. 31:399–405.

Hodgson, T., R. Casais, B. Dove, P. Britton, and D. Cavanagh. 2004. Recombinant infectious bronchitis coronavirus beaudette with the spike protein gene of the pathogenic M41 strain remains attenuated but induces protective immunity. J. Virol. 78:13804–13811.

Jacobson, J. M., L. Feinman, L. Liebes, N. Ostrow, V. Koslowski, A. Tobia, B. E. Cabana, D. Lee, J. Spritzler, and A. M. Prince. 2001. Pharmacokinetics, safety, and antiviral effects of hypericin, a derivative of St. John's wort plant, in patients with chronic hepatitis C virus infection. Antimicrob. Agents Chemother. 45:517–524.

Laconi, A., V. Listorti, G. Franzo, M. Cecchinato, C. Naylor, C. Lupini, and E. Catelli. 2019. Molecular characterization of whole genome sequence of infectious bronchitis virus 624I genotype confirms the close relationship with Q1 genotype. Transbound. Emerg. Dis. 66:207–216.

Leber, B., J. Kale, and D. W. Andrews. 2018. Unleashing blocked apoptosis in cancer cells: new MCL1 inhibitors find their groove. Cancer Discov. 8:1511–1514.

Liang, J. Q., S. Fang, Q. Yuan, M. Huang, R. A. Chen, T. S. Fung, and D. X. Liu. 2019. N-Linked glycosylation of the membrane protein ectodomain regulates infectious bronchitis virus-induced ER stress response, apoptosis and pathogenesis. Virology 531: 48–56.

Liao, Y., T. S. Fung, M. Huang, S. G. Fang, Y. Zhong, and D. X. Liu. 2013. Upregulation of CHOP/GADD153 during coronavirus infectious bronchitis virus infection modulates apoptosis by restricting activation of the extracellular signal-regulated kinase pathway. J. Virol. 87:8124–8134.

Lv, W., C. Liu, Y. Zeng, Y. Li, W. Chen, D. Shi, and S. Guo. 2019. Explore the potential effect of natural herbals to resist newcastle disease virus. Poult. Sci. 98:1993–1999.

Marrelli, M., F. Conforti, C. Toniolo, M. Nicoletti, G. Statti, and F. Menichini. 2014. Hypericum perforatum: influences of the habitat on chemical composition, photo-induced cytotoxicity, and antiradical activity. Pharm. Biol. 52:909–918.

Mirmalek, S. A., M. A. Azizi, E. Jangholi, S. Yadollah-Damavandi, M. A. Javidi, Y. Parsa, T. Parsa, S. A. Salimi-Tabatabaee, H. Ghasemzadeh Kolagar, and R. Alizadeh-Navaei. 2015. Cytotoxic and apoptogenic effect of hypericin, the bioactive component of Hypericum perforatum on the MCF-7 human breast cancer cell line. Cancer Cell Int. 16:3.

Miskovsky, P. 2002. Hypericin-a new antiviral and antitumor photosensitizer: mechanism of action and interaction with biological macromolecules. Curr. Drug Targets 3:55–84.

Mo, M. L., M. Li, B. C. Huang, W. S. Fan, P. Wei, T. C. Wei, Q. Y. Cheng, Z. J. Wei, and Y. H. Lang. 2013. Molecular characterization of major structural protein genes of avian coronavirus infectious bronchitis virus isolates in southern China. Viruses 5:3007–3020.

Montanha, M. C., L. L. Silva, F. B. B. Pangoni, G. B. Cesar, R. S. Gonçalves, W. Caetano, N. Hioka, T. T. Tominaga, M. E. L. Consolaro, A. Diniz, and E. Kimura. 2017. Response surface method optimization of a novel hypericin formulation in P123 micelles for colorectal cancer and antimicrobial photodynamic therapy. J. Photochem. Photobiol. B. 170:247–255.

Naesens, L., P. Bonnafous, H. Agut, and E. De Clercq. 2006. Antiviral activity of diverse classes of broad-acting agents and natural compounds in HHV-6-infected lymphoblasts. J. Clin. Virol. 37:S69–75.

Pu, X. Y., J. P. Liang, X. H. Wang, T. Xu, L. Y. Hua, R. F. Shang, Y. Liu, and Y. M. Xing. 2009. Anti-influenza A virus effect of *hypericum perforatum L.* extract. Virol. Sin. 24:19–27.

Pu, X. Y., J. P. Liang, R. F. Shang, L. Y. Zhou, X. H. Wang, and Y. Li. 2012. Therapeutic efficacy of *hypericum perforatum L.* ex-

tract for mice infected with an influenza A virus. Can. J. Physiol. Pharm. 90:123–130.

Ríos-Ocampo, W. A., T. Daemen, M. Buist-Homan, K. N. Faber, M. C. Navas, and H. Moshage. 2019. Hepatitis C virus core or NS3/4A protein expression preconditions hepatocytes against oxidative stress and endoplasmic reticulum stress. Redox Rep. 24:17–26.

Shih, C. M., C. H. Wu, W. J. Wu, Y. M. Hsiao, and J. L. Ko. 2018. Hypericin inhibits hepatitis C virus replication via deacetylation and down-regulation of heme oxygenase-1. Phytomedicine 46:193–198.

Şimşek, E., E. A. Aydemir, N. İmir, O. Koçak, A. Kuruoğlu, and K. Fışkın. 2015. Dimethyl sulfoxide-caused changes in pro- and anti-angiogenic factor levels could contribute to an anti-angiogenic response in hela cells. Neuropeptides 53:37–43.

Singh, R., A. Letai, and K. Sarosiek. 2019. Regulation of apoptosis in health and disease: the balancing act of BCL-2 family proteins. Nat. Rev. Mol. Cell Biol. 20:175–193.

Şueki, F., M. K. Ruhi, and M. Gülsoy. 2019. The effect of curcumin in antitumor photodynamic therapy: in vitro experiments with Caco-2 and PC-3 cancer lines. Photodiagnosis Photodyn. Ther. 27:95–99.

Sui, X., J. Yin, and X. Ren. 2010. Antiviral effect of diammonium glycyrrhizinate and lithium chloride on cell infection by pseudorabies herpesvirus. Antiviral Res. 85:346–353.

Taher, M. M., G. M. Lammering, C. M. Hershey, and K. C. Valerie. 2002. Mood-enhancing antidepressant St. John's wort inhibits the activation of human immunodeficiency virus gene expression by ultraviolet light. IUBMB Life 54:357–364.

Tang, J., J. M. Colacino, S. H. Larsen, and W. Spitzer. 1990. Virucidal activity of hypericin against enveloped and non-enveloped DNA and RNA viruses. Antiviral Res. 13:313–325.

Westerbeck, J. W., and C. E. Machamer. 2019. The infectious bronchitis coronavirus envelope protein alters golgi pH to protect spike protein and promote release of infectious virus. J. Virol. 93: e00015–19.

Wolfle, U., G. Seelinger, and C. M. Schempp. 2014. Topical application of St. John's wort (Hypericum perforatum). Planta Med. 80:109–120.

Xie, Z., J. Zhang, S. Ma, X. Huang, and Y. Huang. 2017. Effect of Chinese herbal medicine treatment on plasma lipid profile and hepatic lipid metabolism in hetian broiler. Poult. Sci. 96:1918–1924.

Xu, L., X. Zhang, W. Cheng, Y. Wang, K. Yi, Z. Wang, Y. Zhang, L. Shao, and T. Zhao. 2019. Hypericin-photodynamic therapy inhibits the growth of adult T-cell leukemia cells through induction of apoptosis and suppression of viral transcription. Retrovirology 16:5.

Yan, S., J. Zhao, D. Xie, X. Huang, J. Cheng, Y. Guo, C. Liu, Z. Ma, H. Yang, and G. Zhang. 2018. Attenuation, safety, and efficacy of a QX-like infectious bronchitis virus serotype vaccine. Vaccine 36:1880–1886.

Yin, J., G. Li, J. Li, Q. Yang, and X. Ren. 2011. In vitro and in vivo effects of Houttuynia cordata on infectious bronchitis virus. Avian Pathol. 40:491–498.

Yu, L., X. Zhang, T. Wu, J. Su, Y. Wang, Y. Wang, B. Ruan, X. Niu, and Y. Wu. 2017. Avian infectious bronchitis virus disrupts the melanoma differentiation associated gene 5 (MDA5) signaling pathway by cleavage of the adaptor protein MAVS. BMC Vet. Res. 13:332.

Zhai, X. J., F. Chen, C. Chen, C. R. Zhu, and Y. N. Lu. 2015. LC-MS/MS based studies on the anti-depressant effect of hypericin in the chronic unpredictable mild stress rat model. J. Ethnopharmacol. 169:363–369.

Zhang, Z., X. Yang, P. Xu, X. Wu, L. Zhou, and H. Wang. 2017. Heat shock protein 70 in lung and kidney of specific-pathogen-free chickens is a receptor-associated protein that interacts with the binding domain of the spike protein of infectious bronchitis virus. Arch. Virol. 162:1625–1631.

Zhong, Q., Y. X. Hu, J. H. Jin, Y. Zhao, J. Zhao, and G. Z. Zhang. 2016. Pathogenicity of virulent infectious bronchitis virus isolate YN on hen ovary and oviduct. Vet. Microbiol. 193:100–105.

Zhou, X., W. Jiang, Z. Liu, S. Liu, and X. Liang. 2017. Virus infection and death receptor-mediated apoptosis. Viruses 9:E316.